Yan, C., Sagisaka, M., James, C., Rogers, S. E., Alexander, S., & Eastoe, J. (2014). Properties of surfactant films in water-in-CO_2 microemulsions obtained by small-angle neutron scattering. *Journal of Colloid and Interface Science*, *435*, 112-118. https://doi.org/10.1016/j.jcis.2014.08.040

Properties of surfactant films in water-in-CO_2 microemulsions obtained by small-angle neutron scattering

Ci Yan[✧], Masanobu Sagisaka[†], Craig James[†], Sarah Rogers[§], Shirin Alexander[‡] and Julian Eastoe[✧*]

[✧]School of Chemistry, University of Bristol, Bristol BS8 1TS, United Kingdom

[†] Department of Materials Science and Technology, Faculty of Science and Technology, Hirosaki University, Bunkyo-cho 3, Hirosaki, Aomori 036-8561, Japan

§ Rutherford Appleton Laboratory, ISIS Facility, Chilton, Oxfordshire OX11 0QX, United Kingdom

‡ Swansea University, Singleton Park, Swansea, SA2 8PP, United Kingdom

[*] To whom correspondence should be addressed. E-mail: Julian.eastoe@bris.ac.uk

Abstract

Hypothesis

The formation, stability and structural properties of normal liquid phase microemulsions, stabilized by hydrocarbon surfactants, comprising water and hydrocarbon oils can be interpreted in terms of the film bending rigidity (energy) model. Here, this model is tested for unusual water-in-CO_2 (w/c) microemulsions, formed at high pressure with supercritical CO_2 (sc-CO_2) as a solvent and fluorinated surfactants as stabilizers. Hence, it is possible to explore the generality of this model for other types of microemulsions.

Experiments

In this paper, a High pressure Small-Angle Neutron Scattering (HP-SANS) study on w/c microemulsions is described using contrast variation to highlight scattering from the stabilizing fluorinated surfactant films: these data show clear evidence for spherical core-shell structures for the microemulsion droplets.

Findings

The results extend understanding of w/c microemulsions since previous SANS studies are based only on scattering from water core droplets. Here, detailed structural parameters for the surfactant films, such as thickness and film bending energy, have been extracted from the core-shell SANS profiles revealed by controlled contrast variation. Furthermore, at reduced CO_2 densities (~0.7 g cm^{-3}), elongated cylindrical droplet structures have been observed, which are uncommon for CO_2 microemulsions/emulsions. The implications of the presence of cylindrical micelles and droplets for applications of CO_2, and viscosity enhancements are discussed.

Keywords: microemulsions, supercritical CO_2, fluorinated surfactants, film bending rigidity, small-angle neutron scattering

1. Introduction

Supercritical CO_2 ($scCO_2$) has attracted increasing attention as a promising alternative for volatile organic solvents, due to its abundance, non-toxic, non-flammable, and non-hazardous properties which make CO_2 a strong candidate for use as a green solvent. However, due to the low dielectric constant[1,2] (~1.33 at 200 bar, 350 K), $scCO_2$ is generally a very poor solvent, in particular for polar and high molecular weight solutes. On the other hand, emulsions and microemulsions have been widely accepted as effective media to stabilize immiscible components, such as water and oil[3,4]. Studies have been carried out extensively for water-in-$scCO_2$ (w/c) microemulsions over the last two decades, ever since Beckmann et al.[1] suggested that a twin fluorocarbon tailed surfactant should exhibit CO_2 activity. Guided by this hypothesis, Harrison et al.[2] successfully formulated stable w/c microemulsions with H7F7, a hydrocarbon-fluorocarbon hybrid anionic surfactant. A series of fluorinated surfactants have been developed by Sagisaka et.al[5,6,7] based on the structure of Aerosol OT (AOT), a di-chain surfactant which has been widely applied to formulate water in oil microemulsions [3]. Some of these custom designed CO_2 compatible surfactants have exhibited very high efficiencies for stabilization of w/c microemulsions, with the highest water: surfactant ratio (i.e. W=[water]/[surf]) up to 60. Efforts have also been made to formulate hydrocarbon surfactants as cheaper and more environmentally viable substitutes for fluorinated amphiphiles. Experiments with a number of AOT analogues, bearing different oxygenated hydrocarbons have shown promising results[8]. Eastoe et.al[9] have also reported formation of w/c microemulsions with highly branched hydrocarbon surfactants. More work on theoretical studies and practical applications with w/c microemulsions has been described in a number of reviews[10,11,12], and interested readers are referred elsewhere for

details.

Small-Angle Neutron Scattering (SANS) is a powerful technique to study the assembly, alignment, dispersion and mixing of nanoscale condensed matter typically over length scales 1-50 nm [3]. A strength of SANS is the ability to determine statistically significant bulk average particle properties in situ. More importantly, due to the high contrast between different components containing hydrogen (^{1}H) and deuterium (^{2}H), and by controlling isotopic labeling the domains of interest, different nano-compartmentalized systems can be highlighted for detailed analysis[13]. Based on Johnston et al.'s phase studies[2], Eastoe et al[14]. applied High-Pressure SANS (HP-SANS) to D_2O/scCO_2 systems for the first time. A spherical structure was observed for the (micro)emulsified water cores, which provided the first direct evidence for the formation of w/c microemulsions[14]. Having shown the feasibility of using HP-SANS to characterize w/c microemulsions, this technique has been frequently applied in later studies with different surfactants[6,8,15] and structures[16,17,18]. In most of these studies, the microemulsion structures were determined only based on scattering from D_2O cores, and this is due to the difficulty of contrast variation in w/c systems. In particular, isotopic variation with C and O is very expensive, but even though it does not shift the contrast of the eternal CO_2 bulk sufficiently as can be readily done with hydro/deutero-carbons. Although important information such as shape and size of the droplet cores could still be obtained, some of the detailed structural and interfacial properties of the surfactant film in w/c systems remained inaccessible. Recently, Klostermann et al. have investigated a series of CO_2-in-water (c/w) microemulsions stabilized by commercial polydisperse perfluorinted polyethelyneglycol surfactants Zonyl FSN 100 and Zonyl FSO 100[19]. Due to the technical

nature of the surfactants, the exact chemical composition, and therefore, the scattering length densities (SLD) of the surfactants are less well defined. However, contrast variation was performed by mixing heavy and light water (D_2O and H_2O) as the solvent bulk in order to determine the SLD of the surfactant film. In the study, a secondary peak was found on the scattering form factor P(Q) at a H_2O/D_2O composition ratio of ~0.68, which is usually considered as an important feature characteristic of core-shell particles.

This study aims to investigate the core-shell structure of w/c microemulsions in detail by using a similar contrast variation strategy as Klostermann et al.[19]. Here, however chemically pure fluorinated AOT analogue anionic surfactants were used, in contrast to the polydisperse commercial grade non-ionic stabilizers used in ref 17. Using these well-defined systems, SANS was not affected by uncertainties that arise from inter-particle interactions, or complex structures in the surfactant layers. Hence, it has been possible to examine core-shell form factors to generate unique interfacial information which can be compared with literature data on other hydrocarbon-based microemulsions. This current study furthers understanding about w/c microemulsion structures and properties, which is useful for improving design of new CO_2-compatible surfactants and applications of w/c systems.

2. Experimental

2.1 Materials and compositions: Two fluorinated surfactants in the nFS(EO)$_2$ series with n=4 and 6 have been used to formulate w/c microemulsions, their structures are presented in Table.1. The details of surfactant synthesis, purification and characterization can be found elswhere[6]. The concentration of surfactant is quoted in molarity units taking into account the known changes in cell volume as function of CO_2 pressure: (0.017 mol L^{-1} in a 20 ml volume at P = 120 bar increasing to 0.025 mol L^{-1} in 12 ml volume after compression to P = 350 bar, all experiments at 45°C).The composition parameter W = [water]/[surfactant]. All components are obtained with well-defined densities, d_{CO2} =0.68 - 0.91 g cm^{-3} (depending on pressure)[20], and $d_{surfactant}$=1.7 g cm^{-3} as a typical fluorinated compound[21]. From the mass density and bound coherent scattering lengths of the isotopes, the SLD of each component can be calculated and constrained for fitting ($\rho_{surfactant}=3.5\times10^{-6}Å^{-2}$, $\rho_{D2O}=6.3\times10^{-6}Å^{-2}$, $\rho_{CO2}=1.6\times10^{-6}Å^{-2}$ when d_{CO2} =0.68 g cm^{-3}, and $2.3\times10^{-6}Å^{-2}$ when d_{CO2} =0.92 g cm^{-3}) It should be noted that the SLD for the water cores of microemulsion droplets is varied through H_2O/D_2O mixing, and the actual values are noted in appropriate sections below.

Surfactant	Structures
4FS(EO)$_2$	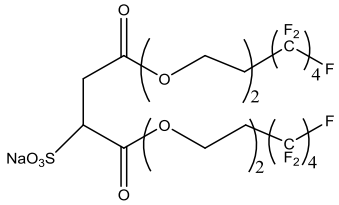
6FS(EO)$_2$	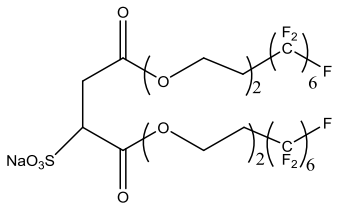

Table 1. Structures of surfactants used.

2.2 Pressure cell: All samples were prepared in a stainless steel cell with variable volume (12-20 ml) controlled by a piston with an external hydraulic pump. Once filled with CO_2, the pressure was measured by a built-in pressure probe with accuracy ±1 bar. Two sapphire windows fitted in parallel allow for visual observations of phase behavior. Temperature was controlled to 45 °C by both a heating circuit and water bath in the cell body.

In order to obtain a w/c microemulsion, an appropriate amount of pre-weighed surfactant and D_2O/H_2O mixture was fed into the cell to establish the molar ratio W (=[water]/[surf]) of interest. Subsequently, the cell was sealed and liquid CO_2 was introduced at ~5°C and re-equilibrated at 45°C in the cell under magnetic stirring. The inlet line was closed once the pressure reached 120 bar, and under these conditions CO_2 has reached a supercritical state. The pressure could be further increased using a hydraulic pump, up to a maximum of 450 (±5) bar, which allowed stable w/c microemulsions to be formulated with different W ratios.

2.3 SANS: SANS measurements were performed using instruments LOQ[22] and SANS2D[23] at the ISIS spallation source, Rutherford Laboratory, UK. Results are presented in terms of the intensity (I(Q)) as a function of scattering vector Q, which is defined as

$$Q = \frac{4\pi}{\lambda} sin\frac{\theta}{2} \qquad (1)$$

where θ is the scattering angle and λ the incident neutron wavelength. SANS2D spans a Q range of $0.002 < Q < 1$ Å^{-1} with neutron wavelength λ of 2.2-10 Å^{-1}, whereas for LOQ, $0.008 < Q < 0.25$ Å^{-1} and λ is within the range 2-14 Å^{-1}. The path length was 10 mm. All scattering data were normalized for the sample transmission, empty cell and solvent background and put on an absolute intensity I(Q)/cm^{-1} scale using standard procedures, resulting in errors in

intensity I(Q) lower than 5%.[24] Once w/c microemulsions were obtained at the appropriate conditions, the systems were equilibrated with stirring for 5 min before SANS measurements were made.

2.4 Scattering Theory: The relationship between scattering vector and intensity I(Q) can be described as follows[25]:

$$\mathrm{I(Q)} = N_p V_p^2 (\Delta\rho^2) P(Q) S(Q) + B_{inc} \qquad (2)$$

N_p is the number concentration of scattering particles, V_p is the particle volume, Δρ is the difference of scattering length density between the scattering body and the solvent, P(Q) is the form factor which describes the internal structure of scattering particles. S(Q) is the structure factor which describes interactions between particles, and B_{inc} is the background incoherent scattering.

It should be noted that the form factor P(Q) is not only dependent on the shape of microemulsion droplets, but also the scattering contrast arising from different scattering length density (SLD, or ρ) between adjacent phases. Moreover, hydrogen and deuterium have very different bound coherent scattering lengths, and therefore, by appropriate deuterium isotopic doping the desired contrast can be highlighted from the core, shell, or the whole droplet, enabling study of specific domains. For w/c microemulsions, however, contrast variation is more difficult than for w/o systems, due to the fact that CO_2 and most CO_2 active surfactants cannot be easily subject to isotopic labeling; hence most studies on such systems are only based on core scattering profiles using pure D_2O as the contrast agent. As a result, important information, such as shell thickness or droplet polydispersity cannot be obtained with confidence from the scattering profile. The data were analyzed by the

fitting program SASview using a spherical core-shell form factor model with a Schultz polydispersity term[26,27]. No structure factor (S(Q)) has been considered due to the low surfactant concentration and low dielectric constant of the CO_2 solvent.

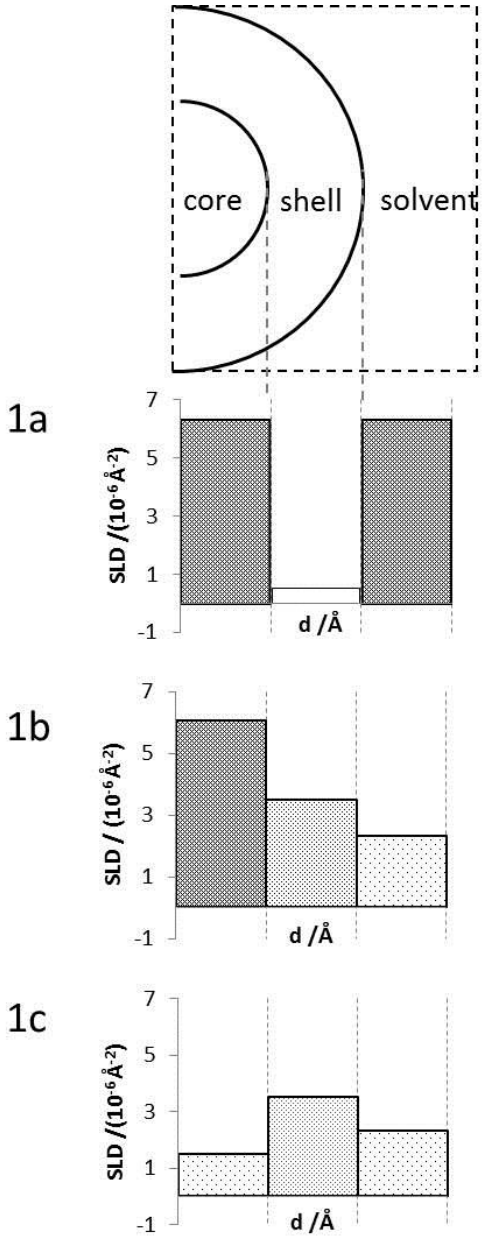

Figure 1. A schematic plot the cross section of a microemulsion droplet, and below the SLD profiles designed for experiments 1a. a typical core-shell structure for hydrocarbon-based w/o microemulsions using D_2O/H-surfactant/D-solvent contrast[3,4]; 1b. D_2O/F-surfactant/CO_2 microemulsion at 350 bar, 45˚C and 1c. the contrast applied in this

work to obtain the core shell structure of w/c microemulsions using mixed H_2O/D_2O.

3. Results and discussion

3.1 Spherical and core-shell systems: Scattering data for the $6FS(EO)_2/scCO_2$ microemulsions doped with D_2O and a H_2O/D_2O mixture (mass ratio 7:3 which gives $\rho_{core}^{SLD}=1.51\times10^{-6}$ Å^{-2}) have been compared at W20. As shown in Figure 2, the nanodroplets with pure D_2O cores scattered with a similar profile as simple spherical particles, whereas for the w/c microemulsions with H_2O/D_2O mixed cores, a core-shell scattering profile was obtained with a distinctive peak at high Q.

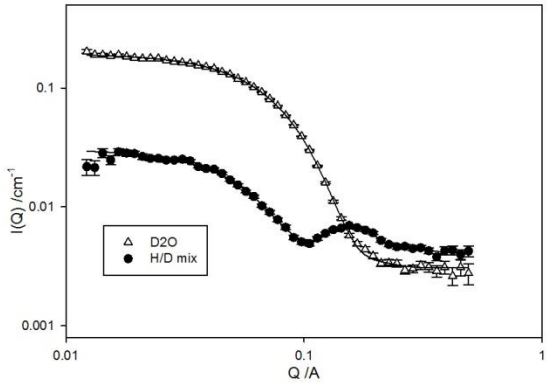

Change to read angstrom -1

Figure 2 Scattering profiles for w/c microemulsions stabilized by $6FS(EO)_2$ at 350 bar, 45˚C. Pure D_2O and a H_2O/D_2O mixture (mass ratio 7:3) was added to each sample giving water: surfactant ratio=20. The scattering data are well fitted with a Schultz core-shell spherical model (lines).

Both scattering profiles can be fitted to a Schultz spherical core-shell model and the fitting parameters are compared in Table 2. Although the structures of the pure D_2O core system are in good agreement with H_2O/D_2O mixed systems, the surfactant layer thickness was

obtained with better precision with from the H_2O/D_2O mixed samples. Furthermore, the uncertainty in polydispersity is also significant with the pure D_2O core systems, as even if manually adjusted in large steps, it does not appear to have significant effect on the fitting.

Core	R_c /Å	Thickness /Å	σ/R_{av}
H/D mixed	20 (±1)	9 (±1)	0.18 (±0.01)
D_2O	19 (±1)	8 (±4)	0.23 (±0.12)*

Table 2. Fit parameters for the w/c microemulsions stabilized by $6FS(EO)_2$ from Figure 2 with two types of core (pure D_2O and a H_2O/D_2O mixture), both systems were analyzed using a spherical core-shell model. As noted in earlier sections, the data are fitted with constrained parameters $\rho_{surfactant}=3.5\times10^{-6}Å^{-2}$, $\rho_{core}=1.5\times10^{-6}Å^{-2}$, $\rho_{CO2}=2.3\times10^{-6}Å^{-2}$**. The adjusted parameters were core radius R_c, thickness and polydispersity** σ/R_{av}**. The volume fraction was also an adjustable parameter, and for both systems ~0.008 was obtained in the fits.**

*** it should be noted again that the errors obtained in the brackets are obtained by fitting the data points with given scattering profiles, though from the actual fitting, the polydispersity could range from 0.2 towards 0.4, giving significant uncertainties.**

3.2 Effect of W ratio: The core-shell structure has been studied for $6FS(EO)_2$ stabilized w/c microemulsions with increasing core radius as water ratio W was increased from 10 to 30 (Figure 3). Using the mixed H_2O/D_2O as water core gave core-shell features in the scattering profiles, and maxima/minima shifting towards lower Q with increasing water content. Interestingly, it has also been found that not only the peak position moves, but also the

intensity of peak increases with core radius.

It should be noted that, the W10 system appears to give a smeared primary and secondary peak, which is attributed to a high polydispersity (σ/R_{av}~0.30) by fitting. However, this may actually due to the limit of resolution for such small core sizes in the examined contrast. In a parallel experiment, a greater core-shell contrast was obtained with reduced core SLD ($\rho_{core}=0.84\times10^{-6}$), and a clear core-shell scattering profile was obtained giving better confidence on the polydispersity σ/R_{av}~0.19. In Figure 3, core radius (R_c) is also plotted as a function of W ratio and is well-fitted to a linear swelling law: the repeat experiment (circled point) gave better consistency compared with the data point below at lower resolution.

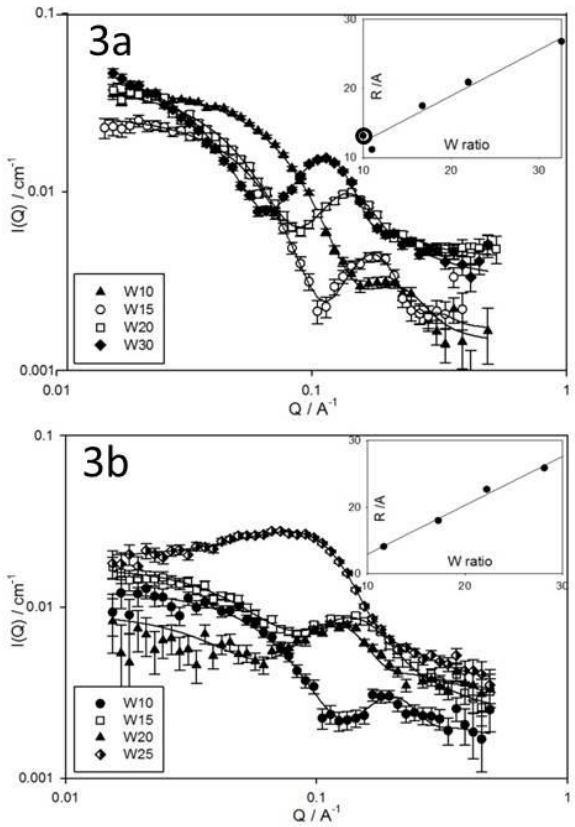

Figure 3. Scattering profiles for w/c microemulsions stabilized by 6FS(EO)$_2$ (3a) and 4FS(EO)$_2$ (3b) with a series of W values. SANS measurements were taken at 350 bar, 45˚C, which is a bulk density d_{CO2} ~0.91 g cm^{-3}. The core radius is also plotted as a function of W

for both systems (the circled data point for 6FS(EO)$_2$ at W=10 was taken from a parallel experiment with enhanced core-shell contrast as described in the main text), and linear correlations were obtained as predicted by a standard spherical swelling law[2,3,28].

3.3 Effect of surfactant chain length: The core-shell structure of w/c microemulsions stabilized by a shorter chain surfactant, 4FS(EO)$_2$, and the changes of intensity between primary and secondary peaks become more significant after addition of water, as compared to the 6FS(EO)$_2$ systems (Figure 3b). Fitted parameters for the contrast variation experiments can be found in Supporting Information (Table S1): but the film thicknesses are 6 Å, i.e. lower than the 9 Å for 6FS(EO)$_2$. This can be explained as a result of increasing relative significance of scattering from the core, which is either enhanced by increasing size of the core relative to the entire particle, or owing to enhanced core-shell contrast (see supporting material, Figure S2). Furthermore, the polydispersity was also found to be higher in general compared to the 6FS(EO)$_2$ stabilized w/c microemulsions, which could be a result of a lower film bending rigidity, as discussed in detail in section 3.5 below.

The radius of w/c microemulsion droplets (R_c) has been plotted against W for both 4FS(EO)$_2$ and 6FS(EO)$_2$ systems, and fitted to a linear swelling law for polydisperse spherical droplets:

$$f\left(\frac{\sigma}{R_{av}}\right) \cdot R_c = \frac{3V_w}{A_h} W + \frac{3V_h}{A_h} \qquad (4)$$

where V_w is the volume of a water molecule, A_h and V_h are the interfacial area and volume per surfactant headgroup, and $f\left(\frac{\sigma}{R_{av}}\right)$ is described as $f\left(\frac{\sigma}{R_{av}}\right) = 1 + 2(\frac{\sigma}{R_{av}})^2$ where $\frac{\sigma}{R_{av}}$ is the polydispersity of microemulsion droplets. The headgroup area was calculated for both surfactant systems giving 133 ± 5 Å^2 for 6FS(EO)$_2$ and $A_h = 108 \pm 5$ Å^2 for 4FS(EO)$_2$, which is in good agreement with literature results, obtained in a similar fashion for fluorinated di-chain surfactant with comparable structures: $A_h = 128 \pm 5$ Å^2 for 8FS(EO)$_2$,[7] and $A_h = 115 \pm 5$ Å^2 for di-HCF4, di-HCF6 and di-CF4.[29] On the other hand, for normal hydrocarbon AOT-stabilized microemulsions in a range of alkane solvents[30], a

mean value of 72 $Å^2$ has been reported for A_h. The smaller A_h value of hydrocarbon (H-carbon) surfactants at w/o interface suggests a higher packing density compared with the fluorocarbon (F-carbon) surfactants at w/c interface, which can be rationalized as an enhanced packing efficiency of F-carbon chains at the w/c interface[40,41].

3.4 Effect of CO_2 bulk density: Variation of pressure, and hence density of $scCO_2$, has also been investigated with the systems discussed above. On reducing bulk density, it might be expected that a more distinguished spherical core-shell structure would be obtained as a result of increasing shell-bulk contrast with lower bulk SLD of CO_2: however, the results show quite the opposite. As presented in Figure 4, for a $6FS(EO)_2$ stabilized w/c microemulsion at W15, the definition of the primary and secondary peak diminished as density was reduced from approximately 0.9 to 0.7 g cm^{-3}; this can be interpreted in terms of increasing polydispersity of the microemulsion droplets (data fitting gives σ/R_{av}~0.32). As the CO_2 density was further decreased down to ~0.68 g cm^{-3} (at 120 bar), the scattering profile is no longer consistent with the spherical core-shell model as previously. Instead, the results can be fitted to a cylindrical model (Figure 5), suggesting that the spherical microemulsion droplets have transformed to elongated structures as a result of reduction in bulk CO_2 density. The effect of pressure on SANS was also examined for a pure D_2O core system and similar results were obtained as for the H_2O/D_2O mixed core systems.

On the other hand, $4FS(EO)_2$ stabilized microemulsions have shown similar behavior at reduced bulk density: at first, no scattering was obtained from the mixture at CO_2 densities below 0.68 g cm^{-3} and the phase appeared turbid. With increasing pressure, a phase transition was observed at ρCO_2 ~0.71 g cm^{-3} (at 130 bar), and similar to $6FS(EO)_2$ systems,

scattering characteristics of anisotropic structures obtained at various W values. It should be noted again that all the SANS data were obtained from w/c microemulsions in transparent single phase regions (visual inspection).

Furthermore, although formation of elongated w/c microemulsions has been reported in a few studies [14-16], this is the first observation of anisotropic micellar structures triggered by changing CO_2 pressure and bulk density. In Table 3, the fitting parameters obtained using the cylindrical form factor model have been compared for w/c systems stabilized by $4FS(EO)_2$ and $6FS(EO)_2$, together with other systems containing cylindrical micelles reported in the literature[11, 15]. Although the aspect ratio between the length and the cross section diameter is significant for the w/c microemulsions, the length appears to be significantly smaller compared with previous observations with different surfactants.

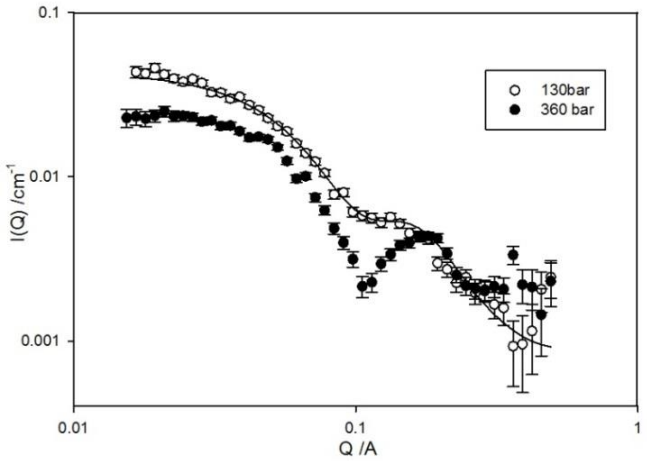

Figure 4. Scattering profiles for $6FS(EO)_2$ stabilized w/c microemulsions at W15, 45˚C; P=130bar and 360 bar(d_{CO2}=0.71 and 0.91 g cm^{-3} respectively).

Change to read angstrom -1

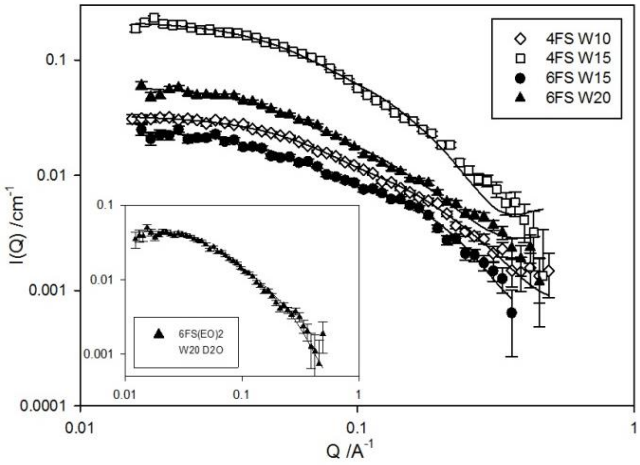

Figure 5. Scattering profiles of w/c microemulsions at different water contents between W10 and W20 at low CO_2 densities (T=45 ˚C, d_{CO2}=0.68 g cm^{-3} and P=120 bar for $6FS(EO)_2$, P=130 bar and d_{CO2}=0.71 g cm^{-3} for $4FS(EO)_2$). The profiles have been fitted to a core-shell cylinder form factor model. It should be noted that, the data/fit for the $4FS(EO)_2$ W15 system has been multiplied by a factor of 4 for clarity of presentation. Also shown in the inset, the scattering profile for a pure D_2O core microemulsion stabilized by $6FS(EO)_2$ under the same experimental conditions.

Surfactants	W	d_{CO2} /(g cm^{-3})	Length (L) /Å	Radius (R)/Å	Thickness /Å	L /2R
$6FS(EO)_2$	15	0.68	50 ±2	3 ±1	6	10
	20	0.68	77 (±3) [78 ±3]	3 (±1) [4]	6 [5]	13 [19]
$4FS(EO)_2$	10	0.71	63±2	3±1	5	10
	15	0.71	71±5	3±1	6	11
TC14+C_2Benz	10	0.91	140±2	17±1	N/A	4
(9:1 ratio)[a]	20	0.91	160±2	23±1	N/A	3.5
TC14+C_4Benz	10	0.91	77±2	15±1	N/A	2.5
(9:1 ratio)[a]	20	0.91	294±2	29±1	N/A	5
Co(di-$HCF_4)_2$ [b]	10	1.00	261±5	11±2	9	7
Ni(di-$HCF_4)_2$ [b]	10	1.00	273±5	10±2	9	7

Table 3. Fitting parameters obtained from the core-shell cylindrical model for w/c microemulsions under reduced CO_2 density. Values in square brackets are for the D_2O contrast only sample, data and fit shown in inset to Figure 5.

***[a] ellipsoidal micelles obtained by James et al. (ref.11) using a CO_2-philic hydrocarbon surfactant TC14 with different added hydrotropes.**

***[b] cylindrical w/c microemulsions obtained by Trickett et al. (ref.15) using a di-chain AOT-analogue fluorinated surfactant with transition metal cations.**

3.5 Droplet polydispersity and film bending rigidity: Film rigidity, or bending energy, is a central parameter in one of the most widely accepted theories accounting for microemulsion stability[29]. In simple terms, it represents the energy required to deform the interfacial film stabilizing the droplets from a preferred curvature, and may be readily accessed through experiments to determine a composite term ($2K + \overline{K}$) where K represents the bending energy (elasticity) and $\overline{K}$ is a factor associated with Gaussian curvature accounting for film topology[31]. Safran[32] and Milner[33] suggested thermally excited interfacial fluctuations could be described in terms of spherical harmonics. This leads to the film rigidity being related to polydispersity of spherical droplets σ/R_{av}, and the entropy of mixing of the microemulsion droplets $f(\phi)$ (Equation 5).

$$2K + \overline{K} = \frac{k_B T}{8\pi(\frac{\sigma}{R_{av}})^2} - \frac{k_B T}{4\pi} f(\phi) \qquad (5)$$

As discussed in earlier sections, the polydispersities have been determined for series of spherical droplet w/c microemulsions by analyzing the core-shell scattering profiles, and based on Equation 5, the film rigidity of these systems can be estimated. (Note, this model has not been applied to the cylindrical microemulsions, such as shown in Figure 5, as equation 5 applies only to spherical systems).

The resulting bending rigidities of $6FS(EO)_2$ and $4FS(EO)_2$ films in w/c microemulsions at d_{CO2} ~0.91 g cm^{-3} have been plotted against W and compared in Figure 6. At first sight, there is little apparent correlation between the film rigidity and water content, however, the results also show that the film rigidities with a longer chain surfactants are generally higher, as on average, $2K + \overline{K} = 1.7\, k_B T$ for $6FS(EO)_2$, and $1.2\, k_B T$ for $4FS(EO)_2$. In previous studies by Klostermann et al[34,35], the film bending rigidity was also determined for bi-continuous

w/c microemulsions using SANS and NSE (Neutron Spin Echo), and owing to the different topology of bi-continuous microemulsions, a different methodology was used, representing a so called 'bare bending rigidity' $\kappa_0 \sim 0.9 k_B T$ for two different polydisperse polymeric F-carbon surfactant films[34,35]. Comparing with the 4- and 6FS(EO)$_2$ stabilized systems, this value appears to be lower, which is possibly owing to the significantly reduced contribution from $\overline{K}$ for the saddle-shaped curvature in bi-continuous microemulsions.

On the other hand, a number of studies on hydrocarbon-based w/o microemulsions stabilized by H-carbon surfactants[36,37,38] have shown that the film bending rigidity scales with the carbon number (C) in the surfactant tails as $2K + \overline{K} \sim C^{2.3}$. In this current study, albeit with only two different chain lengths, a similar correlation has been obtained, however, with a reduced exponent ~1.2 ($C_{4FS(EO)2}$=12 and $C_{6FS(EO)2}$=16). If only CF_2 was considered as the 'effective unit' in the tail, the power would be further reduced to 0.9 ($C_{4FS(EO)2}$=8 and $C_{6FS(EO)2}$=12). Hence, compared with w/o microemulsions, the film bending rigidity in w/c microemulsions seems to be less dependent on surfactant tail carbon number.

It should be noted that, the bending rigidity of 6FS(EO)$_2$ and 4FS(EO)$_2$ films in w/c microemulsions also appears to be higher compared with an H-carbon di-chain surfactant film with comparable a chain length: for example, with water/di-C_n-PC/n-hexanol/iso-octane microemulsions[39], a similar film bending rigidity $\sim 1.7\, k_B T$ was obtained but for a total carbon number C=24. Speculatively, the reasons for difference in $2K + \overline{K}$ between F-carbon (w/c) and H-carbon (w/o) surfactants could be: 1. Enhanced elastic moduli *K* for F-carbon chains owing to higher steric crowding of CF_2 units; 2. As suggested by Rossky et al.[40, 41], the steric density and unfavorable electrostatic interactions in F-carbon films also result in less

penetration of both water and CO_2 molecules through the interface compared with H-carbon analogue w/o systems, which is expected to dampen the fluctuations of the surfactant films: hence, the film bending rigidity increases. 3. With the additional factors mentioned above, surfactant chain length becomes a less dominant factor for the film bending rigidity for water/F-carbon surfactant/scCO_2 microemulsions, as revealed by the scaling $2K + \bar{K} \sim C^{1.5}$ obtained from this study rather than an exponent of 2.3 found for w/o systems[36-39].

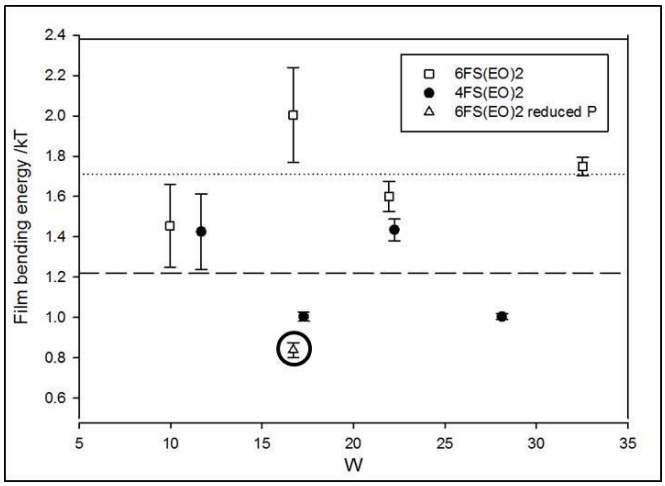

Figure 6. Film bending rigidity in units of k_BT for w/c microemulsions stabilized by 6FS(EO)$_2$ (black dots) and 4FS(EO)$_2$ (white squares) at various W ratios, 350 bar and 45 ˚C. It should be noted that the data point for the 6FS(EO)$_2$ system at W10 was taken from a repeat experiment and the result is more consistent with the others, as suggested in previous sections. The film bending rigidity for the W15, 6FS(EO)$_2$ at lower pressure (130 bar) is also plotted (circled white triangle), a significant reduction can be seen comparing with the high pressure systems.

Furthermore, as CO_2 density was reduced towards 0.71 g cm^{-3} at pressure P=130 bar, the film rigidity has been found to drop significantly to 0.83 k_BT(circled data point in Figure 6), and in the studies by Klostermann et al.[33], a similar trend was also obtained. With further reduction in CO_2 density, the surfactant film rigidity could no longer be obtained for the cylindrical microemulsion droplets using Equation 5, since the correlation is only valid for spherical particles. However, by considering the effect of CO_2 bulk density on the film bending energy as mentioned earlier, it can be deduced that the surfactant film becomes increasingly flexible as the CO_2 density drops, and the elongated structures may also be attributed to this effect.

4. Conclusions

A method has been successfully developed to highlight core-shell structures in water-in-CO_2 microemulsions using contrast variation High Pressure SANS, and the following important features have been revealed:

1. By studying the size polydispersity of w/c microemulsion droplets, film bending energies have been determined for fluorinated surfactants with two different chain lengths. Comparing to the results from w/o microemulsions stabilized by di-chain H-carbon surfactants[36-39], and bicontinuous w/c microemulsions[34,35] stabilized by polydisperse polymeric F-carbon surfactants, the 4- and 6FS(EO)$_2$ surfactant films appear to have higher bending energies, and $2K + \overline{K} = 1.2 \sim 1.7 k_B T$. The film rigidity was also found to scale with surfactant chain carbon number as: $2K + \overline{K} \sim C^{1.2}$, the exponent in this correlation (1.2) is lower than that obtained from H-carbon surfactants in w/o systems(~2.5) [36 - 39].
2. As the CO_2 bulk density is reduced towards the phase instability boundary, the spherical microemulsion droplets were found to elongate and the SANS could be described in terms of cylindrical aggregates. This is the first observation of pressure/density driven shape transitions for w/c microemulsions. Although these cylindrical structures are not sufficiently anisotropic to drive significant viscosity enhancements, this is a very interesting observation which deserves further attention. Instead of changing the chemical compositions in the surfactant film by using designed surface-active additives[18], hydrotropes[16] or chemical methods such as ion exchange in the headgroups[17], the bulk density of scCO_2 could represent a

convenient way to induce shape transitions, which has the potential to open up new applications of CO_2 as a solvent and processing medium.

1 Hoefling TA, Enick RM, Beckman EJ, J Phys Chem 1991; 95: 7127.
2 Harrison K, Goveas J, Johnston KP, O'Rear EA. Langmuir 1994; 10: 3536.
3 Nave S, Eastoe J. Langmuir, 2000; 16: 8741
4 Nave S, Eastoe J, Heenan RK, Steytler D, Grillo I, Langmuir 2002; 18: 1505
5 Sagisaka M, Yoda S, Takebayashi Y, Otake K, Kitiyanan B, Kondo Y, Yoshino N, Takebayashi K, Sakai H, Abe M, Langmuir 2003; 19: 220.
6 Sagisaka M, Yoda S, Takebayashi Y, Otake K, Kondo Y, Yoshino N, Sakai H, Abe M, Langmuir 2003; 19: 8161
7 Sagisaka M, Iwasa S, Hasegawa S, Yoshizawa A, Mohamed A, Cummings S, Rogers SE, Heenan RK, Eastoe J, Langmuir 2011; 27: 5772.
8 Fan X, Ptluri VK, McLeod MC, Wang Y, Liu J, Enick RM, et al. J Am Chem Soc 2005; 127: 11754.
9 Hollamby MJ, Trickett K, Mohamed A, Cummings S, Tabor RF, Myakonkaya O, et al. Angew Chem Int Ed 2009; 48: 4993.
10 Eastoe J, Dupont A, Steytler DC. Curr Opin Colloid Interface Sci. 2003; 8: 267.
11 Eastoe J,Yan C, Mohamed A. Curr Opin Colloid Interface Sci. 2012; 17: 266.
12 James C, Eastoe J. Curr Opin Colloid Interface Sci. 2012; 18: 40
13 Hollamby MJ. Phys.Chem. Chem. Phys., 2013; 15: 10566
14 Eastoe J, Bayazit Z, Martel S, Steytler D C, Heenan R K. Langmuir 1996; 12: 1423
15 Eastoe J, Gold S, Rogers S, Wyatt P, Steytler D C, Gurgel A, et al. Angew. Chem. 2006; 118: 3757
16 James C, Hatzopoulos MH, Yan C, Smith GN, Alexander S, Rogers SE, Eastoe J, Langmuir 2014; 30: 96
17 Trickett K, Xing D, Enick R, Eastoe J, Hollamby MJ, Mutch KJ, et al. Langmuir 2010; 26: 83.
18 Cummings S, Enick R, Rogers S, Heenan R, Eastoe J. Biochimie, 2012; 94: 94.
19 Klostermann M, Strey R, Foster T, Sottmann T, Schweins R, Lindner P, Phys. Chem. Chem. Phys., 2011; 13: 20289
20 McClain J B, Londono D, Combes JR, Romack TJ, Canelas DA, Betts DE, Wignall GD, Samulski ET, DeSimone JM, J. Am. Chem. Soc, 1996; 118: 917.
21 Zielinski R G, Kline S R, Kaler E W, Rosov N, Langmuir, 1997; 13; 3934.
22 Heenan R K, Penfold J, King S M, J. Appl. Crystallogr., 1997; 30: 1140.
23 Heenan R K, Rogers S E, Turner D, Terry A E, Treadgold J K, Neutron News 2011; 22: 19.
24 Wignall G D, Bates F S, J. Appl. Crystallogr. 1987; 20: 28.
25 King S M, Pethrick RA & Dawkins JV (editors), Modern Techniques for Polymer Characterisation, 1999; Chapter 7.
26 Guinier A, Fournet G, Wiley J, Small-Angle Scattering of X-Rays, 1995.
27 Kotlarchyk M, Chen SH, J. Chem. Phys., 1983; 79: 2461.
28 Nave S, Eastoe J, Heenan RK, Steytler DC, Grillo I, Langmuir 2000; 16: 8741
29 Eastoe J, Downer A, Paul A, Steytler DC, Rumsey E, Penfold J, Heenanc RK, Phys. Chem. Chem. Phys., 2000; 2: 5235
30 Eastoe J, Robinson BH, Young WK, Steytler DC, Faraday Trans. 1990; 86: 2883.
31 Eastoe J, Cosgrove T (editor), Colloid Science Principles,methods and applications, Chapter 5.
32 Safran SA, J. Chem. Phys., 1983; 78: 2073
33 Milner ST, Safran SA, Phys. Rev. A, 1987; 36: 4371
34 Klostermann M, Strey R, Sottmann T, Schweins R, Lindner P, Holderer O, Monkenbusch M, Richter D, Softmatter, 2012; 8: 797
35 Holderer O, Klostermann M, Monkenbusch M, Schweins R, Lindner P, Strey R, Richtera D, Sottmann T, Phys. Chem. Chem. Phys., 2011;13:3022
36 Kegel WK, Bodnar I, Lekkerkerker H N W, J.Phys.Chem., 1995; 99: 3272
37 Eastoe J, Sharpe D, Heenan RK, Egelhaaf S, J. Phys. Chem. B 1997;101:944

38 Eastoe J, Sharpe D, Langmuir, 1997;13:3289
39 Eastoe J, Hetherington KJ, Sharpe D, Langmuir, 1997; 13: 2490
40 Stone MT, Rocha SRP, Rossky PJ, Johnston KP, J. Phys. Chem. B 2003; 107: 10185
41 Rocha SRP, Johnston KP, Rossky PJ, J. Phys. Chem. B 2002, 106, 13250-13261